Applied Catalysis B: Environmental 111–112 (2012) 342–348

Contents lists available at SciVerse ScienceDirect

Applied Catalysis B: Environmental

journal homepage: www.elsevier.com/locate/apcatb

Isothermal desulfation of pre-sulfated Pt-BaO/γ-Al_2O_3 lean NOx trap catalysts with H_2: The effect of H_2 concentration and the roles of CO_2 and H_2O

Do Heui Kim[a,b,*], Ja Hun Kwak[a], János Szanyi[a], Charles H.F. Peden[a]

[a] Institute for Integrated Catalysis, Pacific Northwest National Laboratory, 902 Battelle Blvd., Richland, WA 99354, United States
[b] School of Chemical and Biological Engineering, Seoul National University, 1 Gwanak-ro, Gwanak-gu, Seoul 151-742, Republic of Korea

ARTICLE INFO

Article history:
Received 17 March 2011
Received in revised form 7 October 2011
Accepted 11 October 2011
Available online 17 October 2011

Keywords:
Pt-BaO/γ-Al_2O_3
SO_2
Lean NOx trap
Desulfation
H_2S
COS

ABSTRACT

The desulfation mechanisms of pre-sulfated Pt-BaO/γ-Al_2O_3 lean NOx trap catalysts were investigated under isothermal conditions (600 °C) using H_2 as the reductant. Sulfates were found to be reduced first with H_2 to produce SO_2, followed by a reaction between SO_2 and H_2 to produce H_2S. Gas analysis during the rich pulse reveals that the sulfur removal efficiency is initially proportional to the H_2 concentration. At constant H_2 concentration the overall desulfation efficiency decreases in the order of $H_2/CO_2/H_2O > H_2/CO_2 > H_2/H_2O > H_2$, as confirmed by XPS analysis of residual sulfur in the desulfated samples. H_2O limits the evolution of SO_2 at an early stage of the rich pulse and enhances the production of H_2S in later stages of reduction. CO_2 is involved in both the formation of COS and the production of H_2O (via the reverse water–gas shift reaction), therefore, resulting in an increased overall efficiency.

1. Introduction

Operating internal combustion engines (ICE) under lean conditions, i.e., at higher than stoichiometric air to fuel ratios, can significantly improve their fuel efficiencies. This approach guarantees less fuel consumption and, thus, reduced emission of greenhouse gas. Removal of harmful nitrogen oxides (NOx), however, requires the development of new catalyst technologies because conventional three-way catalytic converters, which operate effectively only at stoichiometric air-to-fuel ratios, are unable to reduce NOx from the highly oxidizing exhaust stream. Among the new and only very recently commercialized after-treatment solutions, lean NOx traps (LNT) (also known as NOx storage–reduction (NSR) catalysts), which consist primarily of platinum group metals (Pt-Rh), NOx storage components (BaO or K_2O) and a support material (γ-Al_2O_3), demonstrate excellent performance for the abatement of NOx emissions under lean conditions [1,2]. Despite its outstanding deNOx ability, the catalyst system is prone to poisoning by sulfur oxides present in the exhaust gas stream. Specifically, the NOx-storage component (BaO) reacts readily with sulfur oxides, resulting in the formation of thermodynamically stable sulfates, thus preventing the storage of nitrogen oxides as nitrates [3,4]. Consequently, LNT catalysts gradually deactivate at rates proportional to the levels of sulfur exposure [5]. The desulfation step, a periodic high temperature (>600 °C) reduction process, is required to regenerate the deactivated sulfate containing NOx storage materials.

Due to the importance of understanding sulfation/desulfation processes in developing durable LNT catalytic systems, many groups have performed detailed studies of these processes on Pt-BaO/γ-Al_2O_3 catalysts [6–15]. Most often, these studies have focused on the desulfation process as a function of temperature with the aim of understanding how sulfur can be removed from the catalysts with reductants. For that purpose, H_2 TPRX (temperature programmed reaction with hydrogen) has been generally used as the technique of choice for obtaining information about the reactivity of sulfur-containing species as a function of temperature [3,6,11,16]. H_2 TPRX, however, provides an idealized set of experimental conditions that are typically not present under realistic catalyst operation. A reducing environment is sustained over the entire temperature range, instead of introducing the reducing gases intermittently in the middle of longer lean periods, as is typically done under actual application conditions. Instead, it is useful to experimentally characterize the release of sulfur-containing gases under isothermal conditions where lean/rich desulfation cycles are introduced.

In this work we studied LNT desulfation chemistry under isothermal conditions, by varying the concentration of reductant (H_2), and by evaluating the role of both CO_2 and H_2O in the

* Corresponding author at: Seoul National University, School of Chemical and Biological Engineering, 1 Gwanak-ro, Gwanak-gu, Seoul 151-742, Republic of Korea. Tel.: +82 2 880 1633; fax: +82 2 888 7295.
E-mail address: dohkim@snu.ac.kr (D.H. Kim).

0926-3373/$ – see front matter © 2011 Elsevier B.V. All rights reserved.
doi:10.1016/j.apcatb.2011.10.017

desulfation process. In order to operate the after-treatment system more efficiently, one must optimize the amount of reductant gases, since excessive amounts of reductant will lower the overall fuel economy, while insufficient reductant will result in incomplete desulfation, and thereby severely limiting the NOx uptake capacity of the storage component. In this study hydrogen was chosen as a representative reductant, since it guarantees the most extensive desulfation [17]. Examining the specific roles of CO_2 and H_2O in the desulfation chemistry is also very important, since these gases are always present at high concentrations in the exhaust gas mixtures. Previous studies have revealed that H_2O plays a key role in facilitating desulfation via the hydrolysis of refractory BaS that forms during reduction by H_2 [18]. Furthermore, CO_2 has been shown to promote desulfation by inhibiting the formation of the undesirable BaS phase [19,20]. It is also known that certain sulfur containing gases (e.g. COS) are easily transformed into SO_2 or H_2S by their reaction with H_2O or CO_2 [21].

2. Experimental

A Pt(2 wt%)-BaO(20 wt%)/γ-Al_2O_3 LNT sample was prepared by a conventional impregnation method as described previously [22]. The catalyst was then calcined at 500 °C for 2 h in a 10% O_2/He flow. A "sulfated" sample was prepared by treating a portion (0.7 g) of the calcined LNT sample in a gas mixture (flow rate 190 cc/min) containing both SO_2 (50 ppm) and O_2 (10%) in a balance of He at 300 °C for 24 h. The ratio of S/Ba is about 0.62, assuming that the SO_2 introduced is fully adsorbed on the Ba component of the catalyst, as evidenced by the fact that no SO_2 was observed by mass spectrometry during the sulfation. After sulfur treatment, the sulfated sample was removed from the reactor and mixed to make a number of uniform samples for subsequent desulfation experiments.

To initiate the isothermal desulfation experiments using a portion (0.1 g) of the sulfated sample, the temperature was raised to 600 °C under lean conditions (200 ppm NO, 12% O_2, 10% CO_2 and 10% H_2O balanced with He). After staying at 600 °C for 5 min in the lean gas mixture, desulfation was performed at 600 °C in two sequences (10 min rich/1 min lean) with hydrogen, at varying concentrations (0.1%, 1% and 6%), as the rich reductant. The flow rate under lean or rich conditions is 300 cm^3/min. For the studies of the effects of H_2O and CO_2, their concentrations were maintained at 10%, using constant concentrations of hydrogen of 1%. Finally, the sample was cooled to room temperature in the lean gas mixture after isothermal desulfation, and then prepared for ex-situ analysis with XPS.

During the desulfation at 600 °C, the evolution of gases was followed with a quadrupole mass spectrometer (MS, an MKS Minilab) every 1.4 s. Mass fragments characteristic of SO_2, H_2S, COS, H_2, H_2O and CO_2 gases were monitored at m/e of 64, 34, 60, 2, 18 and 44, respectively. Note that the mass fragment at m/e = 34 also arises from an isotopic variant of molecular O_2 ($^{18}O^{16}O$) that is measureable when O_2 is in the feed gas (lean conditions). However, reductive desulfations were carried out in the absence of O_2 in order to unambiguously measure the production of H_2S.

Ex-situ x-ray photoelectron spectroscopy (XPS) experiments were carried out on desulfated samples in the analysis chamber of a Physical Electronics Instruments Quantum 2000, using Al Kα X-rays and a pass energy of 71 eV. The position and intensity of the Al2 s peak at 119.2 eV were used as references.

3. Results

3.1. Effects of H_2 concentrations

We first investigated the effects of H_2 concentration during rich pulses on desulfation, by varying the H_2 levels (0.1%, 1%–6%), while keeping those of H_2O and CO_2 constant (both at 10%) in the reaction mixture. The results are shown in Figs. 1–4 where the exact timing of the switch from lean to rich conditions (near Time = 0) can be identified in the data by the sharp fall-off of the mass 34 peak. As just discussed in the experimental section, mass 34 arises from both an isotopic variant of molecular O_2 during lean periods, and from the product H_2S during rich periods.

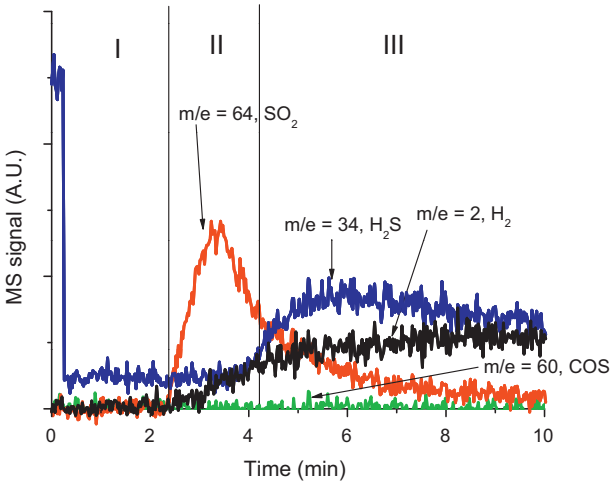

Fig. 1. Mass spectrometer signals of H_2 (m/e = 2), H_2S (m/e = 34), COS (m/e = 60) and SO_2 (m/e = 64) measured during desulfation of a Pt(2 wt%)-BaO(20 wt%)/γ-Al_2O_3 LNT catalyst at 600 °C with a gas mixture containing 10% H_2O, 10% CO_2 and 0.1% H_2 in a balance of He.

Fig. 1 shows the evolution profiles of gases observed during the first rich (10 min) pulse with H_2 concentration of 0.1%. The gas evolution profiles during the rich pulse can be divided into three regions. In the initial stage (I), there is no H_2 MS signal indicating complete H_2 consumption up to 2 min. Based on the H_2 concentration, gas flow rate, and the amount of Pt in the catalyst sample, we can estimate the amount of H_2 consumed is roughly twice the Pt present. While this could indicate complete reduction of PtO_2, we note that reduction of supported Pt can occur at these temperatures without H_2 present. Furthermore, we have no evidence that all Pt has been oxidized to PtO_2 in the prior lean period. Still, the lack of sulfur containing gases during the stage (I) period is good evidence that a significant amount of the H_2 has been consumed to reduce

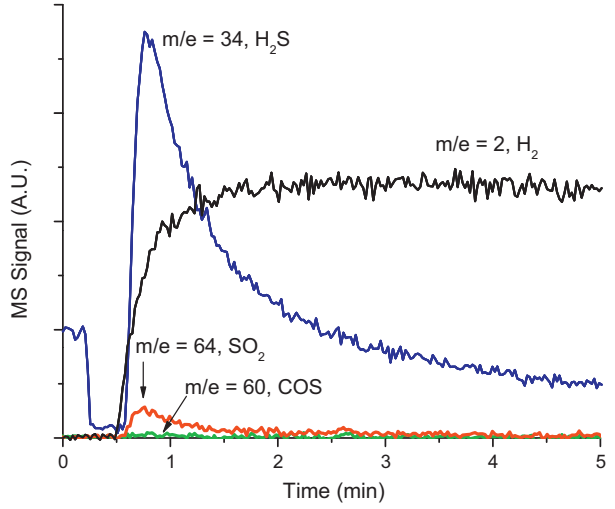

Fig. 2. Mass spectrometer signals of H_2 (m/e = 2), H_2S (m/e = 34), COS (m/e = 60) and SO_2 (m/e = 64) measured during desulfation of a Pt(2 wt%)-BaO(20 wt%)/γ-Al_2O_3 LNT catalyst at 600 °C with a gas mixture containing 10% H_2O, 10% CO_2 and 1% H_2 in a balance of He.

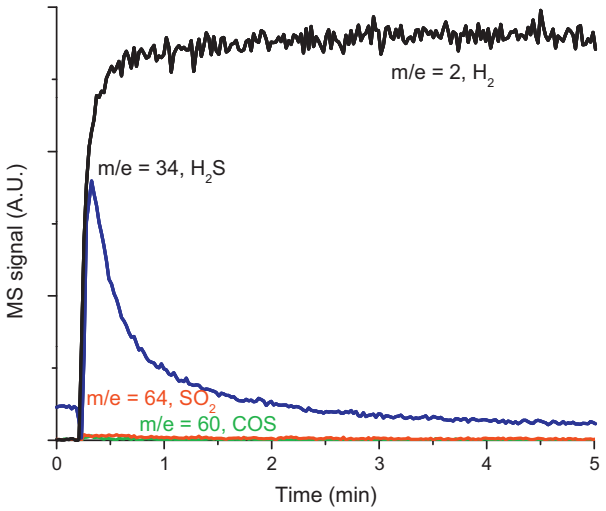

Fig. 3. Mass spectrometer signals of H_2 ($m/e = 2$), H_2S ($m/e = 34$), COS ($m/e = 60$) and SO_2 ($m/e = 64$) measured during desulfation of a Pt(2 wt%)-BaO(20 wt%)/γ-Al_2O_3 LNT catalyst at 600 °C with a gas mixture containing 10% H_2O, 10% CO_2 and 6% H_2 in a balance of He.

PtOx to metallic Pt and also possibly resulting in high concentrations of surface H-atoms from the dissociation of H_2 on the now metallic Pt sites. In the 2nd region (II), H_2 consumption was initially still 100% and SO_2 now appears in the effluent and reaches a maximum concentration around 3 min after the start of the 10 min rich period. SO_2 formation is attributed to the reduction of Ba-sulfate by hydrogen atoms, which are supplied from Pt. In the third region (III), H_2S begins to evolve as the gas-phase SO_2 levels slowly decay to zero. At the same time, the MS signal of H_2 slowly increases with time and stays constant after 6 min, indicating incomplete H_2 consumption in this latter stage of reduction.

Increasing the concentration of H_2 from 0.1% to 1% brings about dramatic changes in the evolution curves, as shown in Fig. 2. In 1% H_2, the duration of stage I is shortened to about 0.5 min as a result of the increased H_2 level, and there is little, if any, evidence for the stage II period. The most noticeable difference in comparison to 0.1% H_2 is that the amount of H_2S increased significantly at the expense of SO_2. As in the case of 0.1% H_2, the evolution of SO_2 preceded that of H_2S, although the time gap between their evolution onsets became significantly shorter. The larger amount of H_2S evolution relative to SO_2 can be explained by the facile conversion of SO_2 on metallic Pt in the presence of an abundant quantity of H_2.

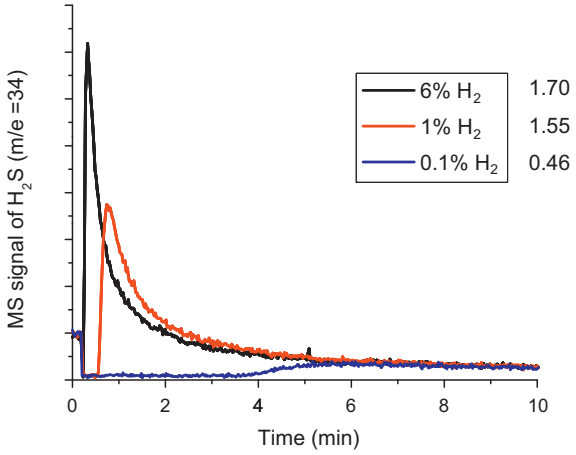

Fig. 4. Comparison of H_2S ($m/e = 34$) signals as a function of H_2 concentration (0.1%, 1% and 6%) during desulfation at 600 °C (from Figs. 1–3).

Table 1
Residual sulfur measured by XPS.

H_2 (%)	0.1	1	6	
S (%)	4.42	3.57	3.65	
1% H_2 + Additional	None	H_2O	CO_2	H_2O/CO_2
S (%)	4.66	4.06	3.91	3.57

When the concentration of H_2 is further increased (to 6%), this trend becomes even more apparent, as the data in Fig. 3 reveals. First of all, in the presence of a large H_2 excess, stage I is now essentially absent. Furthermore, no SO_2 evolution is observed, while the total amount of evolved H_2S slightly increased as the H_2 concentration was increased from 1% and 6%. We note that equilibrium considerations predict that the H_2 concentrations in the gas mixture containing 6% hydrogen can be lowered due to the catalyzed reverse water–gas shift reaction ($CO_2 + H_2 \rightarrow CO + H_2O$) under these particular conditions (0% CO, 6% H_2, 10% CO_2 and 10% H_2O, 600 °C) which gives rise to ~4.8% H_2.

The H_2S evolution profiles obtained at these three different H_2 concentration levels are displayed on the same scale in Fig. 4 for easy comparison. With increasing H_2 concentration, the induction period before the evolution of H_2S becomes shorter and the peak intensity of H_2S get larger. Indeed, when the H_2 concentration is increased from 0.1% to 1%, the total amount of evolved H_2S is increased about 3.4 times. On the other hand, an additional 6 times increase in H_2 concentration (from 1% to 6%) resulted in only about a further 10% increase in the amount of H_2S evolved. For all three cases, note that COS was completely absent in the effluent.

When the amount of H_2 is sufficiently high (e.g. 6% H_2), the evolution of SO_2 is not observed, since any SO_2 formed in the reduction of sulfates is readily consumed by further reacting with H_{ad} on Pt to produce H_2S. Note that, in general, H_2S is the major product rather than SO_2 during H_2 TPRX [3]. The absence of SO_2 in the H_2 TPRX can now be explained by the excess supply of H_2 typically present in this set of experiments. Our isothermal experiments with low H_2 concentration have allowed us to observe the situation when most, if not all of the H_2 is consumed in the rich phases. Very similarly to our results, Epling et al. [23] reported that the ratio of H_2S to SO_2 is increasing with increasing the concentration of H_2 on Pt-based diesel oxidation catalyst.

Because the conversion of SO_2 to H_2S proceeds more efficiently with increasing H_2 concentration, the ratio of H_2S to SO_2 in the effluent is demonstrably related to the H_2 concentrations in the range of 0.1%–6%. However, the total amount of sulfur removed from the catalyst is not directly proportional to the H_2 concentration in the reductant gas mixture. In particular, as evidenced by the XPS data in Table 1, the amount of residual sulfur remaining on the catalyst is relatively unchanged as the hydrogen concentration increases from 1% to 6%. The limited extent of sulfur removal, even under the most favorable reduction conditions, can be rationalized by the extensive sulfation treatment of the LNT catalyst. Under the conditions applied for the preparation of the sulfated Pt/BaO/γ-Al_2O_3 sample, 62% of the base metal oxide (Ba) in the catalyst was converted to sulfates. We suggest that during the desulfation cycle, sulfates at and near the $BaSO_4$/Pt interface are reduced with high efficiency to form SO_2 and then H_2S by atomic hydrogen produced on the Pt surface. As this interface region is depleted in sulfates, the overall reduction rates become diffusion rate-limited; namely, by the diffusion of bulk sulfates to the oxide surface, resulting in a limited extent of desulfation even in a reductant gas mixture containing 6% of H_2.

3.2. Roles of H_2O and CO_2

In order to elucidate the roles of CO_2 and H_2O in the desulfation process with H_2 as the reductant, three experiments were

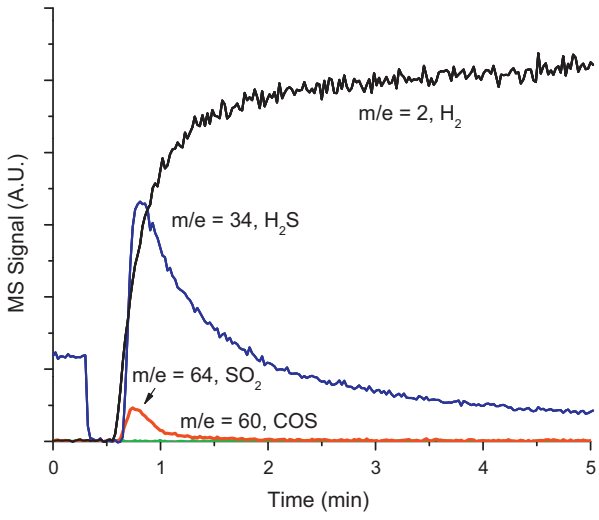

Fig. 5. Mass spectrometer signals of H_2 ($m/e = 2$), H_2S ($m/e = 34$), COS ($m/e = 60$) and SO_2 ($m/e = 64$) measured during desulfation of a Pt(2 wt%)-BaO(20 wt%)/γ-Al_2O_3 LNT catalyst at 600 °C with a gas mixture containing 10% H_2O and 1% H_2 in a balance of He (no CO_2).

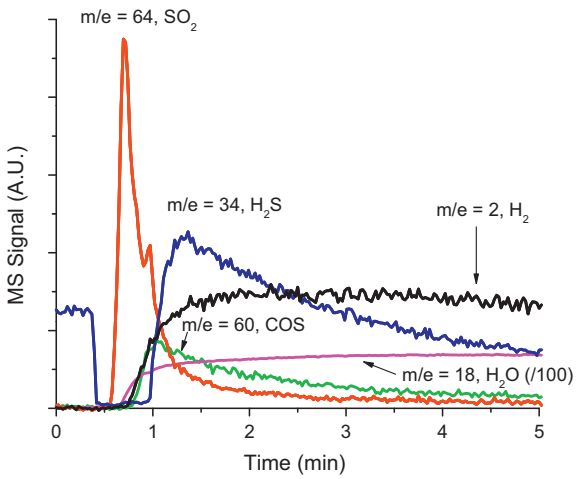

Fig. 7. Mass spectrometer signals of H_2 ($m/e = 2$), H_2S ($m/e = 34$), COS ($m/e = 60$) and SO_2 ($m/e = 64$) measured during desulfation of a Pt(2 wt%)-BaO(20 wt%)/γ-Al_2O_3 LNT catalyst at 600 °C with a gas mixture containing 10% CO_2 and 1% H_2 in a balance of He (no H_2O).

performed at a fixed and intermediate H_2 concentration of 1% in the absence and presence of CO_2 and/or H_2O, and the results are shown in Figs. 5–7.

First, isothermal (600 °C) desulfation was carried out in the presence of 10% H_2O, but with the exclusion of CO_2. The profiles in gas evolution (Fig. 5) obtained in this experiment are very similar to those observed in the 1% $H_2/CO_2/H_2O$ gas mixture (Fig. 2); namely, small amount of SO_2 evolution, followed by large quantities of H_2S. Based on the comparison between the results for $H_2/H_2O/CO_2$ (Fig. 2) and H_2/H_2O (Fig. 5) gas mixtures, CO_2 seems to have minimal effect on the evolution of sulfur containing gases as long as H_2O is present. However, the XPS measurements of residual sulfur remaining on the catalyst (Table 1), as well as integrated H_2S areas during rich phase desulfation, both demonstrate that the full $H_2/H_2O/CO_2$ gas mixture yields a larger removal of sulfur containing species than a H_2/H_2O mixture. Thus, while the timing and distribution of sulfur-containing products is not affected by the presence or absence of CO_2 during humid desulfations, CO_2 does still appear to promote the sulfur removal process.

The role of H_2O in the desulfation process was further studied by comparing the evolution of sulfur-containing gases during

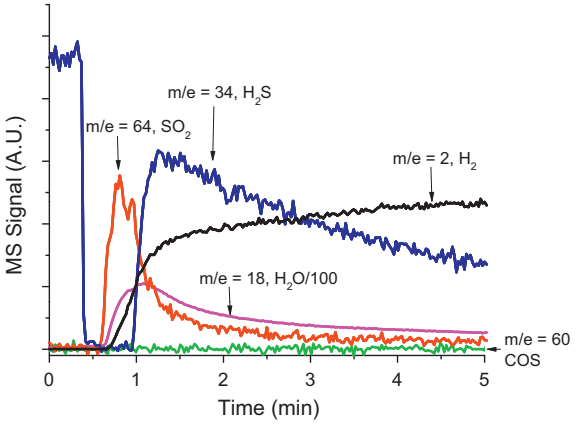

Fig. 6. Mass spectrometer signals of H_2 ($m/e = 2$), H_2S ($m/e = 34$), COS ($m/e = 60$) and SO_2 ($m/e = 64$) measured during desulfation of a Pt(2 wt%)-BaO(20 wt%)/γ-Al_2O_3 LNT catalyst at 600 °C with a gas mixture containing 1% H_2 in a balance of He (no CO_2 and H_2O).

reduction in both the presence (Fig. 5) and absence (Fig. 6) of H_2O at intermediate (1%) H_2 concentrations. When water is present in the gas mixture containing the reductant, H_2S is the primary S-containing product that evolves during desulfation. In the absence of water, however, much larger amounts of SO_2 were evolved, and the appearance of H_2S in the effluent was delayed in comparison to that of SO_2. Furthermore, H_2S appears only after the detection of significant amounts of H_2 and water in the effluent. These observations strongly suggest that water plays an essential role in promoting the conversion of SO_2 to H_2S.

The promotional role of CO_2 for sulfur removal is also evident when H_2O is absent during desulfation. In particular, the results presented in Fig. 7 were obtained for a 1% H_2 and 10% CO_2 gas mixture and demonstrate the evolution sequence of sulfur containing species in the presence of CO_2 but in the absence of H_2O. These results are usefully compared to those in Fig. 6 obtained in the absence of both CO_2 and H_2O. Most remarkable is the large SO_2 evolution at the initial stage of isothermal desulfation. In addition, a new product that was not observed in the other experiments, COS, appears in the effluent as the SO_2 evolution begins to decrease. The rate of COS evolution reaches a maximum at 1 min reduction time and then begins to decrease. As was also observed in Fig. 6, even in the absence of H_2O in the reactant gas mixture, a large amount of H_2O is seen in the effluent. However, unlike the case for desulfation with H_2 alone (Fig. 6), H_2O evolution in the presence of CO_2 (Fig. 7), which appears at approximately the same time as the onset of COS evolution, continues to increase with time likely due to the reverse water–gas shift reaction ($H_2 + CO_2 \rightarrow H_2O + CO$). Similar to the results with H_2 alone, the onset of H_2S evolution shifts to a longer reduction time (to ~1 min) in comparison to desulfation in the presence of H_2O in the reduction gas mixture (compare results of Figs. 2 and 5 with those of Fig. 7). H_2S appears only when significant concentrations of H_2O are observed in the effluent, again indicating that H_2O plays a crucial role in the formation of H_2S.

Fig. 8 more clearly compares the evolution of H_2S and SO_2 during desulfation with and without CO_2 and/or H_2O. The order in the intensity of H_2S peak area (Fig. 8A) is $H_2O/CO_2 > H_2O > CO_2 >$ neither. However, the integrated area of H_2S for the case of H_2/CO_2 is larger than that of H_2/H_2O, due to prolonged production of H_2S at longer desulfation times that results from the formation of H_2O via the reverse water–gas shift reaction. Fig. 8B confirms that the largest amount of SO_2 is evolved when only CO_2 is added to the reductant H_2. The least amounts of

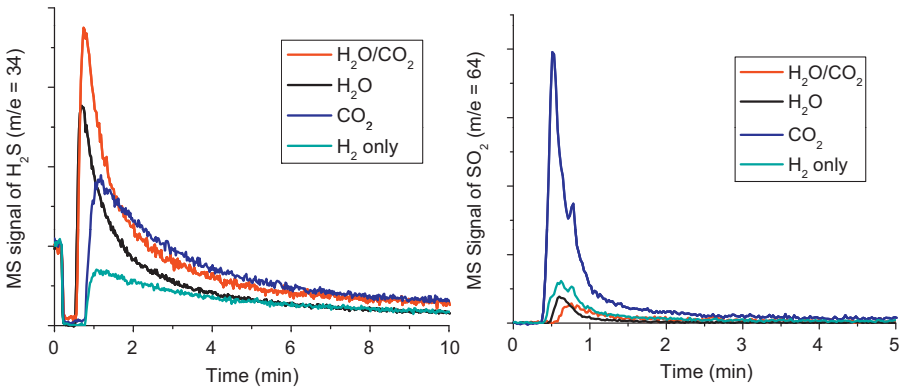

	H_2/H_2O	$H_2/H_2O/CO_2$	H_2/CO_2	H_2
H_2S	1.063	1.545	1.405	0.664
SO_2	0.043	0.076	0.398	0.118

Fig. 8. Comparison of H_2S ($m/e = 34$) and SO_2 ($m/e = 64$) signals during desulfation with 1% H_2 and various reactant gas mixtures (H_2 with both H_2O and CO_2, H_2O, CO_2, or no H_2O and CO_2) at 600 °C (from Figs. 2 and 5–7).

SO_2 were obtained when H_2O was present in the desulfation gas mixture. These results are consistent with those obtained by measuring residual sulfur on the catalyst after these various desulfation treatments as evidenced in Table 1.

4. Discussion

In the following, we discuss the implications of the results obtained here for the mechanisms of desulfation, and the roles played by the various species in the reductant gas mixtures. Note that we do not explicitly discuss reaction "fronts", which arise as the gas composition is changed from lean to rich during desulfation, because they have been discussed extensively in recent literature [24,25]. However, these phenomena are implied by the reaction processes proposed to rationalize the results obtained in this study.

4.1. Effects of H_2 concentrations

Especially informative data regarding the mechanism of the desulfation reaction is obtained when H_2 is present in insufficient quantities, as is the case for the 0.1% H_2 concentration. As evidenced by the lengthy period (stage I) prior to the appearance of any sulfur-containing products during desulfation at these low H_2 concentrations, we conclude that H_2 is first consumed primarily to reduce PtOx clusters to metallic Pt, rather than being used to reduce Ba-sulfates. Subsequently, the metallic Pt provides atomic H (H_{ad} via H_2 dissociation) for the reduction of Ba-sulfates to SO_2. (In the absence of H_2O and perhaps CO_2, over reduction to a highly crystalline form of BaS is also possible as has been shown previously [6]). The thus formed SO_2 can either make it to the exit of the reactor and appear in the effluent, or it can be further reduced to H_2S on metallic Pt surfaces by H_{ad}. As sulfur removal processes are initiated, most of the H_2 is consumed in the conversion of sulfates to SO_2 (note that all of the H_2 is still being consumed when SO_2 first appears). The concentration of SO_2 reaches a maximum coinciding with the appearance of excess H_2 as well as H_2S in the effluent.

The gap in time between the evolution of SO_2 and H_2S can be explained by a consecutive reaction scheme in which Ba-sulfates first react with H_{ad} (from H_2 dissociation on metallic Pt surfaces) to form SO_2, and then the thus formed SO_2 is reduced further downstream by additional H_{ad} on Pt to form H_2S. At the early stage of the desulfation process (when SO_2 evolution is dominant), there is a large amount of sulfates present at or near $BaSO_4$/Pt interfaces. As these sulfates are being reduced by hydrogen atoms formed on the Pt surface, they are desorbed as SO_2 since there is little to no hydrogen left for their further reduction. As the concentration of the easily accessible sulfates decreases, the amount hydrogen that is available to take part in the reduction of SO_2 to H_2S increases, and eventually becomes sufficiently high to initiate this additional reduction process. These processes also readily explain the H_2 concentration dependence displayed in Figs. 1–3. For example, at the highest concentrations studied (6%), there is sufficient H_2 present to carry out all of these sequential reducing processes (i.e., reduction of PtOx, Ba-sulfate, and SO_2 reduction to H_2S), resulting in little to no time gap in the appearance of both H_2 and H_2S in the effluent and essentially no SO_2. We summarize the above discussion with the following reaction equations:

$$PtOx + H_2 \rightarrow Pt + H_2O \uparrow \quad (1)$$

$$Pt + H_2 \rightarrow 2H_{ad}(Pt) \quad (2)$$

$$BaSO_4 + 2H_{ad}(Pt) \rightarrow BaO + H_2O \uparrow + SO_2 \uparrow \quad (3)$$

$$Pt + SO_2 \rightarrow Pt\text{-}SO_{2ad} \quad (4)$$

$$Pt\text{-}SO_{2,ad} + 6H_{ad}(Pt) \rightarrow H_2S \uparrow + 2H_2O \uparrow \quad (5)$$

4.2. Roles of H_2O and CO_2

Next, we discuss the roles for H_2O and CO_2 in the reductive desulfation processes. When neither H_2O nor CO_2 are fed into the reductant stream (Fig. 6), SO_2 and H_2S come out sequentially through the reactions (4) and (5). The behavior is quite similar to that observed at much lower H_2 concentrations of .1% (Fig. 1). Note also that the total amount of sulfur containing species evolved in the absence of both CO_2 and H_2O is much less than in the other cases (Fig. 8 and Table 1). Both of these results suggest a strong promotional role for H_2O and/or CO_2 in the desulfation reaction with H_2.

Specific roles for H_2O in the desulfation processes are evident by comparing results in Figs. 5 and 6. While the onset of sulfur containing products is only marginally affected by the presence of water, the sulfur product distributions are markedly changed. Notably, the primary desulfation product in the presence of H_2O is H_2S rather than SO_2. When H_2 concentrations are somewhat low, first PtOx is reduced followed by reduction of Ba-sulfates that are

in the vicinity of Pt particles and, therefore, more readily removed. As this initially creates a relatively large concentration of SO_2 and a depletion of H_2, SO_2 is the observed product of desulfation followed by H_2S. Another important change during the desulfation with H_2 alone is the conversion of substantial amounts of barium sulfate into a BaS phase [6]. In the presence of H_2O, however, the formed BaS can readily react with H_2O [18] and, thus, account for the additional production of H_2S (Fig. 5) compared with desulfation in H_2 only (Fig. 6). The arguments can be made to rationalize the enhanced overall removal of sulfur (Fig. 8 and Table 1) during desulfation in the presence of H_2O.

The promotional role for CO_2 appears to be somewhat more complex as highlighted in Fig. 7. Even if H_2O is not added in the reactants, the reverse water–gas shift reaction (see reaction (6) below) can operate to produce H_2O and, therefore, give rise to the just described H_2O promotion of desulfation. The equilibrium constant for the reverse water–gas shift reaction (6) at 600 °C is about 0.4, so that the concentrations of H_2O and CO would result in 0.82% in the presence of 1% of H_2 and 10% CO_2. It means that significant amount of H_2O and CO is formed during the reductive treatment at 600 °C even if H_2O and CO are not added initially. The formation of CO can be confirmed by the evolution of COS during the desulfation step, as seen in Fig. 7.

Furthermore, as evidenced especially in Fig. 8B, is a considerably enhanced production of SO_2 at the early stages of desulfation. Indeed, a promotional role for CO_2 in the decomposition of even the more "refractory" Ba-sulfates at long desulfation times may explain the continued and, ultimately, greater production of H_2S (Fig. 8) relative to that observed in the absence of CO_2. This conclusion is also supported by the post-reaction XPS data contained in Table 1. Finally, another significant difference in the results shown in Fig. 7 is the opening of a new channel for desulfation via the formation of COS as a reaction product. We suggest that CO, which is produced from the reverse water–gas shift reaction, readily reacts with SO_2 to generate COS, as has been reported in a previous publication [26]. Thus, the following two reactions describe additional processes that can occur when both H_2 and CO_2 are present in the desulfation gas mixture; reactions that are evident in the absence of H_2O.

$$H_2 + CO_2 \leftrightarrow H_2O + CO \quad (6)$$

$$SO_2 + 3CO \rightarrow COS + 2CO_2 \quad (7)$$

With regard to the sulfur-containing product, COS (Fig. 7, reductant gas = H_2 and CO_2), two other experimental results are worth considering. First is the observation in Fig. 7 that the evolution of COS reaches a peak value rapidly and then quickly decays as the concentrations of H_2O and H_2S continue to increase. Additionally, recall again that COS is only observed when H_2O is absent from the reductant gas mixture (compare Figs. 2 and 7). We suggest that this behavior can be understood by invoking an additional process, the hydrolysis of COS to H_2S [21], as described in Reaction (8):

$$COS + H_2O \rightarrow H_2S + CO_2 \quad (8)$$

The overall efficiency of sulfur removal, as a function of the composition of the desulfation gas mixture (H_2 concentration and the presence of CO_2 and H_2O), can be estimated on the basis of the comparative amounts of H_2S and SO_2 tabulated in Fig. 8 as well as the XPS analysis of the samples prior to and following the desulfation process (Table 1). When both CO_2 and H_2O are present in the reductant gas mixture, the amount of sulfur remaining on the catalyst is very similar for H_2 concentrations of 1 and 6%, while the sample reduced in 0.1% H_2 contains much larger amounts of residual sulfur. This may suggest that under the given desulfation conditions, 1% H_2 is optimal for efficient sulfur removal. Indeed, for 0.1% H_2 concentrations the sulfur removal efficiency is relatively low, while for 6% H_2 a large amount of excess H_2 is measured at the reactor effluent. For 1% H_2 concentrations, the amount of residual sulfur changes in the following order:

$$H_2/H_2O/CO_2 > H_2/CO_2 > H_2/H_2O > H_2$$

This order, evidenced by the results in Table 1, is fully consistent with the amounts of sulfur-containing gases measured during the desulfation process (Fig. 8).

In summary, H_2O and CO_2 play crucial roles in enhancing the desulfation of LNT catalysts. When both H_2O and CO_2 are present along with the reductant H_2, the efficiency for removing sulfur is highest. Under the conditions studied here, somewhat better promotion by CO_2 than H_2O was observed. This result is likely due to multiple roles for CO_2 in enhancing desulfation, which includes the promotion of Ba-sulfate decomposition to SO_2, and the availability of a new desulfation reaction pathway to COS. Furthermore, H_2O promotion is still possible with CO_2 because H_2O is a product of the reverse water–gas shift reaction. One of the roles of H_2O is to promote the reduction of SO_2 to H_2S which is also carried out by the H_2 reductant.

5. Conclusions

Lean NOx trap (LNT) desulfation mechanisms were studied by applying the isothermal (600 °C) reaction with H_2 over pre-sulfated Pt-BaO/Al_2O_3 LNT catalysts as a function of H_2 concentrations and the presence of H_2O and/or CO_2. Desulfation with H_2 then proceeds via SO_2 production, followed by the secondary conversion of SO_2 to H_2S. With increasing H_2 concentrations, the amount of SO_2 decreases since there is now sufficient H_2 available to consume SO_2, thus resulting in a higher H_2S/SO_2 ratio in the reactor effluent. At low H_2 concentrations, the various mechanistic steps of desulfation are most apparent. Notably, the reduction of Pt-oxides, formed during the lean NOx uptake process, appears to be necessary for the initiation of desulfation, as evidenced by a delay in sulfur products at low H_2 concentrations. The efficiency of removing sulfur increases with H_2 concentration, and then levels off. The dependence of sulfur removal on the composition of the reductant gas mixture can be summarized as: $H_2/CO_2/H_2O > H_2/CO_2 > H_2/H_2O > H_2$, as evidenced by post-reaction XPS analyses, as well as quantification of the amounts of sulfur-containing gases. H_2O plays a role in enhancing the conversion of SO_2 to H_2S. The roles of CO_2 involve the formation of COS and the production of H_2O via a reverse water–gas shift reaction, and therefore, resulting in a somewhat higher overall efficiency of desulfation than for the case of H_2O only. Finally, we find that CO_2 significantly enhances to decomposition of Ba-sulfates to SO_2.

Acknowledgements

The authors would like to thank Mark Engelhard for help with the XPS measurements. We also greatly appreciate the referees' suggestions about possible quantitative correlations in our data that were most useful in revising our initial submission, and especially to one reviewer for some specific thermodynamic estimates. Financial support, provided by the U.S. Department of Energy (DOE), Office of Freedom Car and Vehicle Technologies, is also gratefully acknowledged. This work was performed in the Environmental Molecular Sciences Laboratory (EMSL) at Pacific Northwest National Laboratory (PNNL). The EMSL is a national scientific user facility and supported by the U.S. DOE, Office of Biological and Environmental Research. PNNL is a multi-program national laboratory operated for the U.S. Department of Energy by Battelle Memorial Institute under Contract DE-AC06-76RLO 1830.

References

[1] W.S. Epling, L.E. Campbell, A. Yezerets, N.W. Currier, J.E. Parks, Catalysis Reviews Science and Engineering 46 (2004) 163–245.
[2] Z.M. Liu, S.I. Woo, Catalysis Reviews Science and Engineering 48 (2006) 43–89.
[3] F. Rohr, S.D. Peter, E. Lox, M. Kogel, A. Sassi, L. Juste, C. Rigaudeau, G. Belot, P. Gelin, M. Primet, Applied Catalysis B Environmental 56 (2005) 201–212.
[4] L. Lietti, P. Forzatti, I. Nova, E. Tronconi, Journal of Catalysis 204 (2001) 175–191.
[5] P. Engstrom, A. Amberntsson, M. Skoglundh, E. Fridell, G. Smedler, Applied Catalysis B Environmental 22 (1999) L241–L248.
[6] D.H. Kim, J. Szanyi, J.H. Kwak, T. Szailer, J. Hanson, C.M. Wang, C.H.F. Peden, Journal of Physical Chemistry B 110 (2006) 10441–10448.
[7] Y. Su, M.D. Amiridis, Catalysis Today 96 (2004) 31–41.
[8] Z.Q. Liu, J.A. Anderson, Journal of Catalysis 228 (2004) 243–253.
[9] H. Abdulhamid, E. Fridell, J. Dawody, M. Skoglundh, Journal of Catalysis 241 (2006) 200–210.
[10] D.H. Kim, J.H. Kwak, J. Szanyi, S.J. Cho, C.H.F. Peden, Journal of Physical Chemistry C 112 (2008) 2981–2987.
[11] X.Y. Wei, X.S. Liu, M. Deeba, Applied Catalysis B Environmental 58 (2005) 41–49.
[12] A. Amberntsson, M. Skoglundh, S. Ljungstrom, E. Fridell, Journal of Catalysis 217 (2003) 253–263.
[13] S. Elbourazzaoui, E.C. Corbos, X. Courtois, P. Marecot, D. Duprez, Applied Catalysis B Environmental 61 (2005) 236.
[14] J. Dawody, M. Skoglundh, L. Olsson, E. Fridell, Journal of Catalysis 234 (2005) 206–218.
[15] J. Dawody, M. Skoglundh, L. Olsson, E. Fridell, Applied Catalysis B Environmental 70 (2007) 179–188.
[16] D.H. Kim, J. Szanyi, J.H. Kwak, X.Q. Wang, J. Hanson, M. Engelhard, C.H.F. Peden, Journal of Physical Chemistry C 113 (2009) 7336–7341.
[17] S. Poulston, R.R. Rajaram, Catalysis Today 81 (2003) 603–610.
[18] D.H. Kim, J.H. Kwak, X.Q. Wang, J. Szanyi, C.H.F. Peden, Catalysis Today 136 (2008) 183–187.
[19] D.H. Kim, J.H. Kwak, J. Szanyi, X.Q. Wang, M.H. Engelhard, C.H.F. Peden, Topics in Catalysis 52 (2009) 1719–1722.
[20] J.P. Breen, M. Marella, C. Pistarino, J.R.H. Ross, Catalysis Letters 80 (2002) 123–128.
[21] P.D.N. Svoronos, T.J. Bruno, Industrial and Engineering Chemistry Research 41 (2002) 5321–5336.
[22] J.H. Kwak, D.H. Kim, T. Szailer, C.H.F. Peden, J. Szanyi, Catalysis Letters 111 (2006) 119–126.
[23] J.Y. Luo, D. Kisinger, A. Abedi, W.S. Epling, Applied Catalysis A General 383 (2010) 182–191.
[24] J.S. Choi, W.P. Partridge, C.S. Daw, Applied Catalysis B Environmental 77 (2007) 145–156.
[25] J.S. Choi, W.P. Partridge, J.A. Pihl, C.S. Daw, Catalysis Today 136 (2008) 173–182.
[26] P.D. Clark, N.I. Dowling, M. Huang, W.Y. Svrcek, W.D. Monnery, Industrial and Engineering Chemistry Research 40 (2001) 497–508.